Journal of Sound and Vibration (1999) **221**(1), 67–84
Article No. jsvi.1998.1974, available online at http://www.idealibrary.com.on IDEAL

NON-LINEAR VIBRATION ANALYSIS OF THE COUPLED TEXTILE/ROTOR SYSTEM BY FINITE ELEMENT METHOD

C.-G. CHIEN

Department of Mechanical Engineering,
Chien Hsin College of Technology & Commerce, *Chung-Li*, *Taiwan* 32023, *R.O.C.*

AND

R.-F. FUNG AND C.-L. TSAI

Department of Mechanical Engineering, *Chung Yuan Christian University*,
Chung-Li, *Taiwan* 32023, *R.O.C.*

(*Received* 28 *May* 1998, *and in final form* 14 *September* 1998)

This paper presents the dynamic responses of the coupled textile/rotor system by finite element analysis. When textile is wound either on or off the rotor, the system is non-conservative because mass, inertia and eccentricity of the unbalance of rotor change with time, and also the length of textile is time-dependent. Both the time-varying equations for textile and the whirling vibrations for rotor are derived by Hamilton's principle. It is a moving boundary problem since the unknown length of textile has to be determined as a part of the solutions. The special finite element formulations are developed by applying a complete linear polynomial approximation. The number of elements is fixed while the size of the element changes with time. The Runge–Kutta method is used to obtain numerical results. The effects of constant and non-constant angular rotating speeds, shaft stiffness and non-linear terms on the transient amplitudes of the textile and the whirling deflection of the shaft are investigated.

1. INTRODUCTION

Travelling string-like systems have broad applications in the areas of chemical, textile, computer, and tape recorder industries as well as in many other processes. Such systems involve wires, threads, and other materials with negligible bending rigidity, a straight and unsagged equilibrium configuration. Much research on the vibration behavior of string-like problems has been studied previously [1–3]. These studies considered the string system to have a fixed length and no axial motion. Survey papers by Mote [4] and Abrate [5] presented a picture of the state of the art in the vibration and dynamic stability of the axially moving strings or beams. Although string-like systems exhibit movement, the interest of such studies is still in the fixed length consideration.

0022–460X/99/110067 + 18 $30.00/0

For the problem of a vibration string with time-varying length, Kotera and Kawai [6] analyzed free vibrations of a string with time-varying lengths by Laplace transformation. It should be noted that methods of solving the problems necessarily differ from the classical methods of treating the fixed length problems. For instance, the concepts of natural modes and frequencies become meaningless because as the length of string varies, the natural frequencies become time-dependent and the independence of natural modes of oscillation is lost. While in theory the motion of a string with a variable length can be described to any desired degree of approximation by an infinite system of differential equations, the mathematical difficulty usually becomes prohibitive for all but the first few orders of approximation.

The problems involving the oscillations and the influence of reactive force on the motion of a textile machine rotor on which the textile is wound up were presented in a series of papers by Cveticanin [7–9]. With a new procedure based on the Krylov–Bogoliubov method, Cveticanin [10] observed the dynamic behavior of a rotor with variable parameters and small non-linearity. The dynamics of a rotor with variable mass are given by Bessonov [11]. Usually, the rotor consists of a disk which is symmetrically mounted at the middle of the shaft, and the elastic force in the shaft is assumed to be non-linear. The mass of the shaft is negligible in comparison to that of the disk. The mass of the rotor varies with time due to winding on and off the band. Cveticanin [12] studied the textile machine rotor with constant angular velocity. The above-mentioned papers only concentrated on the vibration of the rotor. As far as non-linear vibrations are concerned, little work has appeared on the subject to coupling oscillations of the textile/rotor system. The purpose of this paper is to investigate the dynamic behavior of the whole system, which consists of an axially moving textile and a whirling rotor. The coupled equations for the textile/rotor system are derived by Hamilton's principle. A special finite element scheme is used to predict the dynamic responses since the Jeffcott rotor has variable mass, inertia and unbalance magnitude. We present the numerical results including the time-dependent length of the textile and the time-dependent radius of the disk. The effects of angular rotating speed, shaft stiffness, and non-linear terms on the transient amplitudes are investigated for the coupled system.

2. SYSTEM DESCRIPTION

The coupled textile/rotor system is shown in Figure 1(a). Two fixed co-ordinate systems xoy and XoY are used to describe the dynamic configuration. The Jeffcott rotor model investigated here is similar to that used by Vance and Lee [13]. It consists of a single, centrally located, unbalanced disk and an orthotropically elastic shaft, running on two rigid bearings. The shaft is assumed massless as compared with the large massive disk. The bearing supports are assumed to be rigid, with the shaft providing all the flexibility. The generalized coordinate r is chosen to describe the whirling oscillation of the rotor system which has a constant angular velocity ω. Since the rotor is whirling, the textile length is time-dependent. The transverse vibration of the textile is in the interval $0 \leqslant x \leqslant l(t)$. The textile

is subjected to an initial tension T and has simple supports as its boundary points $x = 0$ and $l(t)$.

Since the connection point $x = l(t)$ is common to the disk and textile, this point on the textile has the same velocity and acceleration as that in the tangential

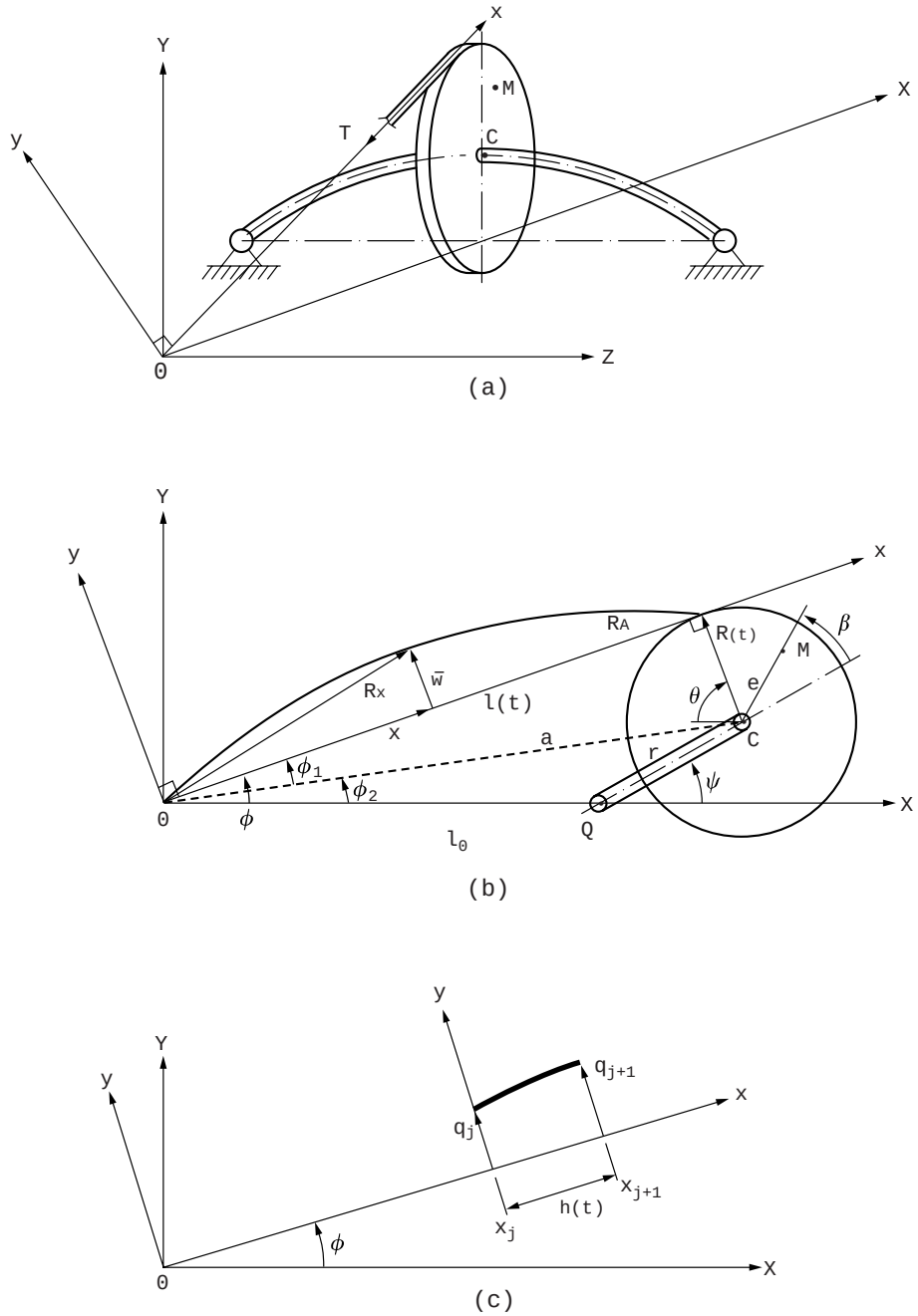

Figure 1. (a) Model of the coupled textile/rotor system. (b) Physical configuration of the coupled textile/rotor system. (c) The deformed element coordinate system.

direction of the disk. It is seen from Figure 1(b) that as the textile is wound on, the disk rotates in a clockwise direction and the shaft angular velocity ω is negative.

The function of the rotor is to wind the textile on or off, so the rotor mass changes with time. In Figure 1(b), $R(t)$ is the radius of the disk, and ψ is the rotary angle. The textile is subjected to an initial tension T, which acts along the tangent line of the disk in the undeformed configuration. The point $x = l(t)$ is one connection point between the textile and rotor. The two vectors, $\mathbf{R_A(t)}$ and $\mathbf{R(t)}$, are perpendicular at point A. From the geometry of Figure 1(b), the time-varying length of the textile is given by

$$l(t) = \sqrt{l_0^2 + r^2 + 2l_0 r \cos\psi - R^2(t)}. \tag{1}$$

The rotor is modelled as a rigid disk mounted on a massless shaft which is supported by two perfect rotating bearings. During winding the textile on or off the disk, the effective mass and radius of the disk vary. The mass $m(t)$ and radius $R(t)$ are assumed to be as given in the papers by Cveticanin [7] and Bessonov [11],

$$m(t) = m_0 - R_1 \rho \omega t, \tag{2}$$

$$R(t) = \left(R_0^2 - \frac{R_1 h \omega t}{\pi} \right)^{1/2}, \tag{3}$$

where m_0 and R_0 are, respectively, the mass and radius of the disk without textile, $R_1 = R_0 + (h/2)$, h is the average thickness of the textile, ω is the angular velocity of the rotor and has a negative value for winding up the textile, and t is time. The unbalance is given by the distance $e = CM$, where C is the geometric center of the disk and M is its mass center, as given by Bessonov[11]:

$$e(t) = -\frac{2}{m_0} R_1^2 \rho \sin\frac{\omega t}{2}. \tag{4}$$

The co-ordinate r gives the magnitude of shaft deflection, and the time derivative $\dot{\psi}$ gives the whirling speed. The instantaneous angular location of the unbalance with respect to the plane of the shaft bending is given by β. Considering the rotor in synchronous vibration, the angle β remains constant. Thus, the whirling speed equals the shaft speed, $\dot{\psi} = \omega$.

3. FINITE ELEMENT DISCRETIZATION

The textile length $l(t)$ is time-dependent when the rotor rotates. Thus, the finite element method carried out for the fixed-size domain is not practical in general because it requires a very large number of small elements. Literature on an axially moving beam develops a more elegant approach element with a varying domain was given by Stylianou and Tabarrok [14]. In this paper, we adopt this concept and use a variable-domain element and the number of elements remains fixed.

3.1. VIBRATIONAL TEXTILE

From Figure 1(b), the position vector of any point on the textile after deformation is

$$\begin{aligned}\mathbf{R}_x(t) &= \mathbf{x} + \mathbf{w} \\ &= (x\cos\phi - w\sin\phi)\mathbf{i} + (x\sin\phi + w\cos\phi)\mathbf{j},\end{aligned} \tag{5}$$

where **i**, **j** are unit vectors corresponding to X and Y components, respectively. $w = w(x, t)$ is the deflection of the textile, and ϕ is the rotary angle of the textile.

The Lagrangian function for the textile is the kinetic energy minus the potential energy. Thus, we have

$$\begin{aligned}L_s &= \frac{1}{2}\int_0^{l(t)} \rho \frac{D\mathbf{R}_x}{Dt}\cdot\frac{D\mathbf{R}_x}{Dt}\,\mathrm{d}x - \int_0^{l(t)} (T\varepsilon_E + \tfrac{1}{2}EA\varepsilon_E^2)\,\mathrm{d}x \\ &= \frac{1}{2}\int_0^{l(t)} \left\{\rho\left[\dot\phi^2 x^2 + 2\dot\phi^2 x\frac{\mathrm{d}w}{\mathrm{d}t} + \left(\frac{\mathrm{d}w}{\mathrm{d}t}\right)^2 + \dot x^2 - 2\dot\phi\dot x w + \dot\phi^2 w^2\right]\right. \\ &\quad \left. - Tw_x^2 - \tfrac{1}{4}EAw_x^4\right\}\mathrm{d}x,\end{aligned} \tag{6}$$

where ρ is the string mass per length, $\varepsilon_E = (1/2)w_x^2$ is the engineering strain, EA denotes the rigidity of the textile, $T\varepsilon_E$ and $(1/2)EA\varepsilon_E^2$ are respectively the terms due to initial tension and deflection. The latter is measured from the initially tensioned configuration.

In order to develop the finite element equation for the string with time-dependent length, we divide the entire length $[0 \leqslant x \leqslant l(t)]$ of the string into N elements. Each element has an equal length $h(t)$ as shown in Figure 1(c). The Lagrangian function for the jth element is then given by

$$\begin{aligned}L_j = \frac{1}{2}\int_{x_j}^{x_{j+1}} &\left\{\rho\left[\dot\phi^2 x^2 + 2x\dot\phi\frac{\mathrm{d}w}{\mathrm{d}t} + \left(\frac{\mathrm{d}w}{\mathrm{d}t}\right)^2\right.\right. \\ &\left.\left. + \dot x^2 - 2\dot x\dot\phi w + \dot\phi^2 w^2\right] - Tw_x^2 - \frac{EAw_x^4}{4}\right\}\mathrm{d}x.\end{aligned} \tag{7}$$

In the process of integrating equation (7), with a finite element discretization shown in Figure 1(c), the transverse deflection of the travelling string is modelled by a complete linear polynomial as

$$w(x, t) = [N(x, l(t))]\{q(t)\}, \tag{8}$$

where

$$\{q(t)\} = \begin{Bmatrix} q_j(t) \\ q_{j+1}(t) \end{Bmatrix},$$

$$[N] = \begin{bmatrix} \dfrac{x_{j+1} - x}{x_{j+1} - x_j} & \dfrac{x - x_j}{x_{j+1} - x_j} \end{bmatrix}$$

$$= \frac{n}{l(t)} \left[\left(l(t) \frac{j+1}{n} - x \right) \left(x - l(t) \frac{j}{n} \right) \right]. \tag{9}$$

It is worth noting that the shape function vector $[N]$ is time-dependent by virtue of the length $l(t)$ changing with time. In order to evaluate $\mathrm{d}w/\mathrm{d}t$ and w_x for the element Lagrangian function (7), we use equation (8) and perform the total differentiation to obtain

$$w_x = [B]\{q\}, \qquad \frac{\mathrm{d}w}{\mathrm{d}t} = [N_t]\{q\} + \dot{x}[B]\{q\} + [N]\{\dot{q}\}, \tag{10}$$

where $[B] = [N_x]$ and the dot indicates partial differentiation of time with respect to t.

Substituting (10) and (8) into (7),

$$L_j = \tfrac{1}{2}\{\dot{q}^{\mathrm{T}}[m_j]\dot{q} + \dot{q}^{\mathrm{T}}[c_{1j}]q + q[c_{2j}]\dot{q}^{\mathrm{T}} + q^{\mathrm{T}}[k_{1j}]q + q^{\mathrm{T}}[k_j]q + [f_{nj}]q + [f_{1j}]q + [f_{2j}]\dot{q} + \dot{f}^2(x)^2 + \dot{x}^2\}. \tag{11}$$

where

$$[m_j] = \int_{x_j}^{x_{j+1}} \rho(N^{\mathrm{T}}N)\,\mathrm{d}x,$$

$$[c_{1j}] = \int_{x_j}^{x_{j+1}} \rho(\dot{x}N^{\mathrm{T}}B + N^{\mathrm{T}}N_t)\,\mathrm{d}x, \qquad [c_{2j}] = \int_{x_j}^{x_{j+1}} \rho(\dot{x}B^{\mathrm{T}}N + N_t^{\mathrm{T}}N)\,\mathrm{d}x,$$

$$[k_{1j}] = \int_{x_j}^{x_{j+1}} (-TB^{\mathrm{T}}B)\,\mathrm{d}x,$$

$$[k_j] = \int_{x_j}^{x_{j+1}} \rho(\dot{x}^2B^{\mathrm{T}}B + \dot{x}B^{\mathrm{T}}N_t + \dot{x}N_t^{\mathrm{T}}B + N_t^{\mathrm{T}}N_t + \dot{\phi}N^{\mathrm{T}}N)\,\mathrm{d}x,$$

$$[f_{nj}] = \int_{x_j}^{x_{j+1}} -\frac{1}{8}EA(qB^{\mathrm{T}}Bqq^{\mathrm{T}}B^{\mathrm{T}}B)\,\mathrm{d}x,$$

$$[f_{1j}] = \int_{x_j}^{x_{j+1}} \rho[2x\dot{\phi}(\dot{x}B + N_t) - 2\dot{x}\dot{\phi}N]\,\mathrm{d}x, \qquad [f_{2j}] = \int_{x_j}^{x_{j+1}} \rho(2x\dot{\phi}N)\,\mathrm{d}x$$

in which $[f_{nj}]$ represents the non-linear term. For the detailed integrations of these coefficient matrices please see the Appendix.

3.2. WHIRLING ROTOR

The Lagrangian function for the rotor is

$$\begin{aligned} L_r = {} & \tfrac{1}{2}m\{[\dot{r} - e(\dot{\psi} - \dot{\beta})\sin\beta + \dot{e}\cos\beta]^2 + [r\dot{\psi} + e(\dot{\psi} + \dot{\beta})\cos\beta + \dot{e}\sin\beta]^2\} \\ & + \tfrac{1}{2}I\dot{\psi}^2 - \tfrac{1}{2}k_x r^2\cos^2\beta - \tfrac{1}{2}k_y r^2\sin^2\beta \\ & - mg[r\sin(\psi + \beta) + e\sin(\psi + \beta)], \end{aligned} \tag{12}$$

where k_x and k_y are shaft stiffnesses in the X and Y directions respectively. It should be noted that the mass m, inertial I and eccentricity e of the rotor are functions of time. However, eccentricity was considered constant as in Fung and Shieh [15].

In order to derive the virtual work done by the initial tension T on the rotor, the virtual displacement at the connection pont will be obtained first. The position vector of the connection point can be written as

$$\mathbf{R}_A(t) = (l_0 + r\cos\psi - R(t)\cos\theta)\mathbf{i} + (r\sin\psi + R(t)\sin\theta)\mathbf{j}. \tag{13}$$

The virtual displacement of the connection point is

$$\delta\mathbf{R}_A(t) = (\delta r\cos\psi + R(t)\sin\theta\delta\theta)\mathbf{i} + (\delta r\sin\psi + R(t)\cos\theta\delta\theta)\mathbf{j}. \tag{14}$$

Since θ is not the generalized co-ordinate chosen to describe the dynamic whirling, $\delta\theta$ should be replaced by δr. To obtain the required relationship, we note from Figure 1(b) that $\theta = (\pi/2) - \phi$. Hence we have $\delta\theta = -\delta\phi$ and the following geometrical relation:

$$\begin{aligned} \sin\phi &= \sin(\phi_1 + \phi_2) \\ &= \frac{R(t)}{a}\cos\phi_2 + \frac{r\sin\psi}{a}\cos\phi_1 \\ &= \frac{1}{a^2}[R(t)(l_0 + r\cos\psi) + l(t)r\sin\psi], \end{aligned} \tag{15}$$

where $a = \sqrt{l_0^2 + r^2 + 2l_0 r\cos\psi}$ is the auxiliary line. Taking the virtual angular displacement from equation (15), we have

$$\delta\phi = C_r\delta r, \tag{16}$$

where

$$\begin{aligned} C_r = {} & \frac{\left[(R(t)\cos\psi + \dfrac{1}{l(t)}(r + l_0\cos\psi)r\sin\psi + l(t)\sin\psi\right]}{[l(t)(l_0 + r\cos\psi) - R(t)r\sin\psi]} \\ & - \frac{2(r + l_0\cos\psi)[R(t)(r + l_0\cos\psi) + l(t)r\sin\psi]}{a^2[l(t)(l_0 + r\cos\psi) - R(t)r\sin\psi]}. \end{aligned} \tag{17}$$

Equation (16) states the relationship between $\delta\phi$ and δr.

The initial tension vector is

$$\mathbf{T} = -T(\cos\phi\mathbf{i} + \sin\phi\mathbf{j}). \tag{18}$$

The virtual work done by the initial tension can be expressed as

$$\begin{aligned}\delta W &= \mathbf{T}\cdot\delta\mathbf{R}_A(t)\\ &= T[\cos\psi\cos\phi - \sin\psi\sin\phi + C_r R(t)]\delta r.\end{aligned} \tag{19}$$

3.3. FORMULATION FOR THE COUPLED TEXTILE/ROTOR SYSTEM

To obtain the equations for the coupled system, the calculus of variation and Hamilton's principle are employed. However, the application of the principle is not straight-forward, since there is a moving boundary involved at $x = l(t)$. It is seen from equation (1) that the length $l(t)$ will be determined when the rotor deflection r is obtained.

We consider the entire system including the textile with length $0 \leqslant x \leqslant l(t)$ and the rotor. Hamilton's principle can be written as

$$\int_{t_1}^{t_2}\left[\delta\int_0^{l(t)} L_s(x, t; w, w_x, w_t)\,\mathrm{d}x + \delta L_r(t; r, \dot{r}) + \delta W\right]\mathrm{d}t = 0, \tag{20}$$

where t_1 and t_2 are two arbitrary end times. We consider the string including the entire length $[0 \leqslant x \leqslant l(t)]$ and use N elements in the finite element discretization. Taking variation of equation (20), applying integration by part, using Leibnitz's law, and collecting the like terms, we obtain

$$\begin{aligned}0 = \int_{t_1}^{t_2}\Bigg\{&L_s[l(t), t; w(l(t), t)]\delta l(t) + \sum_{j=1}^{N}\left[\frac{\partial L_j}{\partial q} - \frac{\mathrm{d}}{\mathrm{d}t}\left(\frac{\partial L_j}{\partial\dot{q}}\right)\right]\delta q\\ &+\left(\frac{\partial L_r}{\partial r} - \frac{\partial}{\partial t}\frac{\partial L_r}{\partial\dot{r}} + T[\cos\psi\cos\phi - \sin\psi\sin\phi + C_r R(t)]\right)\delta r\Bigg\}\,\mathrm{d}t\\ &+\left[\sum_{j=1}^{N}\frac{\partial L_j}{\partial\dot{q}}\,\delta q + \frac{\partial L_r}{\partial\dot{r}}\,\delta r\right]_{t_1}^{t_2}.\end{aligned} \tag{21}$$

The varied path coincides with the true path at the two end points t_1 and t_2. It follows that $\delta w(t_1) = \delta w(t_2) = 0$ and $\delta r(t_1) = \delta r(t_2) = 0$. In the variation process, $\delta l(t)$ exists in the first term of equation (21) because the position $x = l(t)$ is not specified. From equation (1), we also have

$$\delta l(t) = \frac{1}{l(t)}(r + l_0\cos\psi)\delta r. \tag{22}$$

Substituting equation (22) into the first term of equation (21), and collecting them with the $(\partial L_r/\partial r - \partial/\partial t\, \partial L_r/\partial \dot{r})\delta r$ term, we can obtain the Lagrange equations for the textile and rotor respectively, as

$$\sum_{j=1}^{N}\left[\frac{\partial L_j}{\partial q} - \frac{\mathrm{d}}{\mathrm{d}t}\left(\frac{\partial L_j}{\partial \dot{q}}\right)\right] = 0, \tag{23}$$

$$\frac{\partial L_r}{\partial r} - \frac{\partial}{\partial t}\frac{\partial L_r}{\partial \dot{r}} + T[\cos\psi\cos\phi - \sin\psi\sin\phi] + \frac{1}{l(t)}(r + l_0\cos\phi)\cdot L_s[l(t), t; w(l(t), t)] = 0. \tag{24}$$

In deriving the element equation, we isolate a typical element from the mesh and formulate the variational problem by using its finite element model. Then, coefficients of the assembled matrix can be obtained directly. The assembled global equations for the string and rotor are, respectively,

$$[M]\ddot{Q} + [C]\dot{Q} + [K]Q = -[F] - [F_n], \tag{25}$$

$$\begin{aligned}\ddot{r} + \frac{\dot{m}}{m}\dot{r} + \left[\frac{k_x}{m}\cos^2\beta + \frac{k_y}{m}\sin^2\beta - \omega^2\right]r \\ = e\omega^2\cos\beta + 2\dot{e}\omega\sin\beta + e\frac{\dot{m}}{m}\dot{\phi}\sin\beta - \dot{e}\frac{\dot{m}}{m}\cos\beta \\ - \ddot{e}\cos\beta - g\sin\psi - \frac{T}{m}[\cos\psi\cos\phi - \sin\psi\sin\phi] \\ - \frac{(r + l_0\cos\phi)}{2m\ell(t)}[\rho\dot{x}^2 + \rho\dot{x}^2 w_x^2(l(t), t) - T w_x^2(l(t), t) - \tfrac{1}{4}EA w_x^4(l(t), t)],\end{aligned} \tag{26}$$

where

$$[M] = \sum_{j=1}^{N}[m_j], \qquad [C] = \sum_{j=1}^{N}[c_j^*], \qquad [K] = \sum_{j=1}^{N}[k_j^*],$$

$$[F] = \sum_{j=1}^{N}[f_j^*], \qquad [F_n] = \sum_{j=1}^{N}[f_{nj}], \qquad Q = [q_1, q_2, \ldots, q_n]^{\mathrm{T}},$$

$$[c_j^*] = [c_{2j}] - [c_{2j}]^{\mathrm{T}} - [\dot{m}_j], \qquad [k_j^*] = [k_j] + [k_{1j}] - [\dot{c}_{2j}], \qquad [f_j^*] = \frac{[f_{1j}] - [\dot{f}_{2j}]}{2}.$$

Equations (25) and (26) are the non-linear, second order differential equations with variable coefficients. $[K]$ and $[M]$ matrices correspond respectively to the well-known stiffness and mass matrices of the string. $[F]$ matrix is caused by the gyroscopic effect of the moving string. $[F_n]$ matrix is caused by the non-linear terms of the deflections.

From the governing equations (25) and (26), some observations are made as follows:

(i) The mass $m(t)$, inertia $I(t)$ and the eccentricity $e(t)$ of the unbalance of the rotor are time-varying when the textile is wound on or off.

(ii) In this paper, longitudinal elastic deformation of the textile is neglected, and so every point of the textile has the same axial traveling velocity $\dot{x}$ and acceleration $\ddot{x}$, which are given by

$$\dot{x} = -R(t)\dot{\psi}, \qquad 0 < x < l(t), \tag{27a}$$

$$\ddot{x} = -\dot{R}(t)\dot{\psi} - R(t)\ddot{\psi}, \qquad 0 < x < l(t). \tag{27b}$$

In equations (27a, b), the shaft deflection r is very small compared to $R(t)$ and is hence neglected in this study.

(iii) The axial travelling velocity $\dot{x}$ has a positive value as the textile moves along the positive x-axis direction. In the case of constant angular velocity of the shaft, the radius $R(t)$ of the disk and the axial velocity $\dot{x}$ of the textile are non-linear functions of time. Meanwhile, $\dot{R}(t)$ is not equal to zero and the axial travelling acceleration $\dot{x}$ also exists.

(iv) The term $[F]$ in equation (25) is the whirling effects of the rotor on the textile vibration. The terms including $w_x(l(t), t)$ in equation (26) and the end effect at $x = l(t)$ of the textile vibration on the rotor whirling. From equation (10) and zero node displacement $q_{N+1} = 0$ at $x = l(t)$, we have $w_x(l(t), t) = B_N q_N$. Thus, equations (25) and (26) can be combined together in a matrix form and to be solved.

(v) The terms containing EA in equations (25) and (26) are due to the geometric non-linearity of the textile. If they are neglected for the small-amplitude transverse vibrations of the textile, the governing equation (25) becomes linear. However, equation (26) is still non-linear due to the moving boundary at $x = l(t)$.

(vi) The emphasis is placed on the moving boundary condition of the coupled textile/rotor system. The connection point $x = l(t)$ is not specified and its position moves with time. The boundary position $x = l(t)$ will be solved simultaneously with equations (25) and (26).

To solve the problem, the Runge–Kutta numerical method will be used to integrate equations (25) and (26) for the transient solutions.

4. NUMERICAL RESULTS AND DISCUSSION

Since the amplitudes of the textile/rotor system are governed by two non-linearly coupled equations (25) and (26) with time-dependent coefficients, an analytical solution is not possible. The examples given here are chosen to demonstrate the effectiveness of the variable-size element, and to discuss the dynamic responses of the textile/rotor system when the angular velocity ω of rotor is accelerated, decelerated and taken as a periodic perturbation. Finally, we also make a comparison between the linear and non-linear effects on the transient

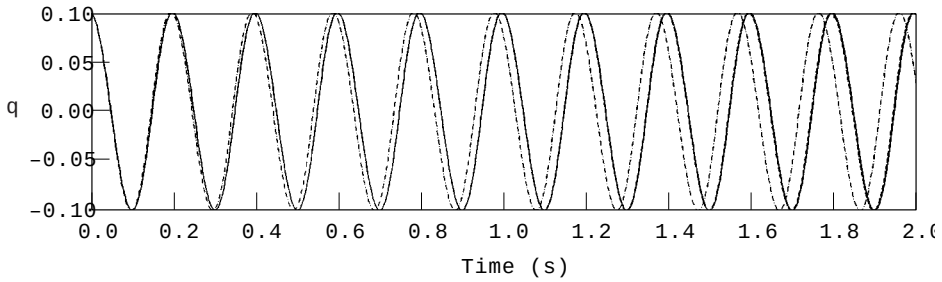

Figure 2. Middle deflections of the string for various element numbers [$N = 4$ (–·–·–), $N = 10$ (——), $N = 12$ (——)].

amplitudes of the textile, the whirling deflection of the rotor, and the time-dependent textile length and the disk radius.

In Figure 2, numerical results show the transient displacements of the string at the middle point by taking element numbers $N = 4$, 10 and 12. In this figure, we simplify the dynamic equations (25) and (26) by setting the rotor at rest, $\omega = 0$. The other parameters are: $T = 100$ N, $\rho = 1$ kg/m, $l_0 = 1$ m, $R_0 = 0$ m and $EA = 0$. The initial displacement is a sine wave with amplitude 0·1 m. It is well known that the period is 0·2 s. For economy in computing time and desired accuracy 10^{-9} to match the period 0·2 s well, we take element number $N = 10$ in the following studies even though many more elements will provide better accuracy.

In Figure 3, we show the coupling effect on the transient vibrations of the textile/rotor system as the rotor rotates with an angular speed $\omega \neq 0$. The parameter values are: $T = 100$ N, $\rho = 1$ kg/m, $l_0 = 1$ m, $m_0 = 4{\cdot}95$ kg, $R_0 = 0{\cdot}1$ m, $h = 0{\cdot}02$ m, $e(t) = -(2/m_0)R_1^2\rho \sin(\omega t/2)$ and the values of shaft stiffness are chosen as $k_x = k_y = 493\,430$ N/m. We consider the textile and rotor with the zero initial conditions: $q_i(0) = 0$, $\dot{q}_i(0) = 0$, $i = 2, 3, \ldots, N$, and $r(0) = \dot{r}(0) = 0$. The results with the angular velocities $\omega = -\pi$ (dash line) and $\omega = -2\pi$ (solid line) are compared in Figure 3. The transient amplitudes of the textile at middle point are shown in Figure 3(a). It is noted that the amplitude builds up and then diminishes in a regular pattern. A beating phenomenon may occur, since the forcing frequency is close to, but not exactly equal to, the natural frequency of the string system. We have also noted that the force term [F] has a strong influence on the amplitude of the string. It is found that the amplitudes with $\omega = -2\pi$ are larger than those with $\omega = -\pi$. Figure 3(b) shows the transient whirling vibrations of the shaft. Figure 3(c) shows the textile length decreases with time. Figure 3(d) shows the rotor radius $R(t)$ increases with time. Figure 3(e) and (f) show the angular velocity $\dot{\phi}$ and acceleration $\ddot{\phi}$ of the string, both exhibiting a beating phenomenon.

In Figure 4, we make a comparison for the rotary angular velocity $\omega = -10 + 2\cos(\Omega_f t)$ with $\Omega_f = \pi c_2/l_0\sqrt{1 - v_0/c_2}$ and $\Omega_f = 2\pi c_2/l_0\sqrt{1 - v_0/c_2}$. The other parameters are the same as those in Figure 3. It is observed that the amplitudes of both the textile and rotor are larger and fluctuate more excitedly when the rotary angular velocity $\Omega_f = 2\pi c_2/l_0\sqrt{1 - v_0/c_2}$. It can seen that the system is unstable.

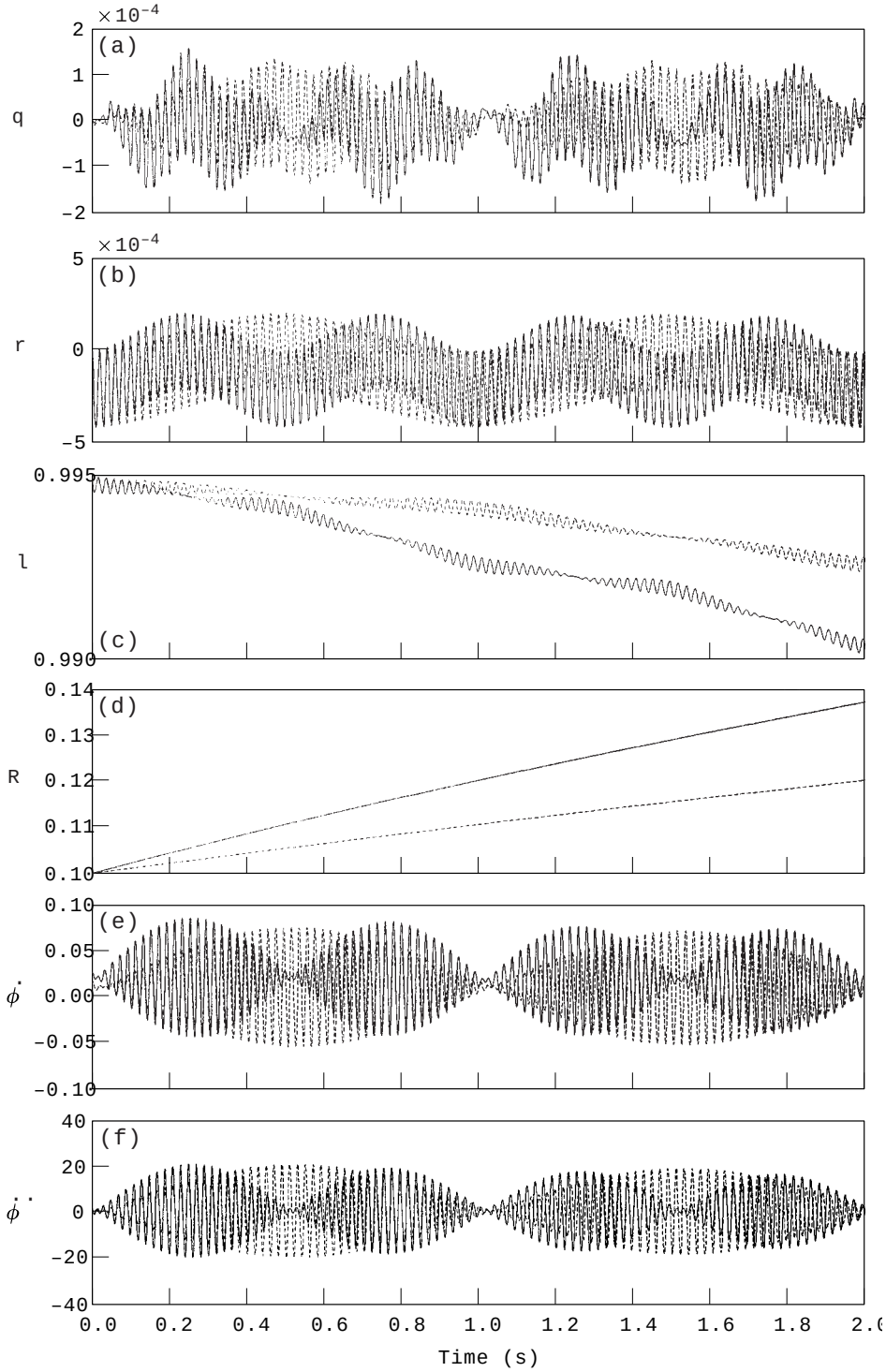

Figure 3. Influence of angular speed of rotor on the transient amplitudes for the case, $\omega = -\pi$ (– – –); $\omega = -2\pi$ (——). (a) Middle deflections of the textile. (b) The deflections of the shaft. (c) Time-dependent length l of the textile. (d) Time-dependent radius R of the disk. (e) Time history of angular velocity $\dot{\phi}$. (f) Time history of angular acceleration $\ddot{\phi}$.

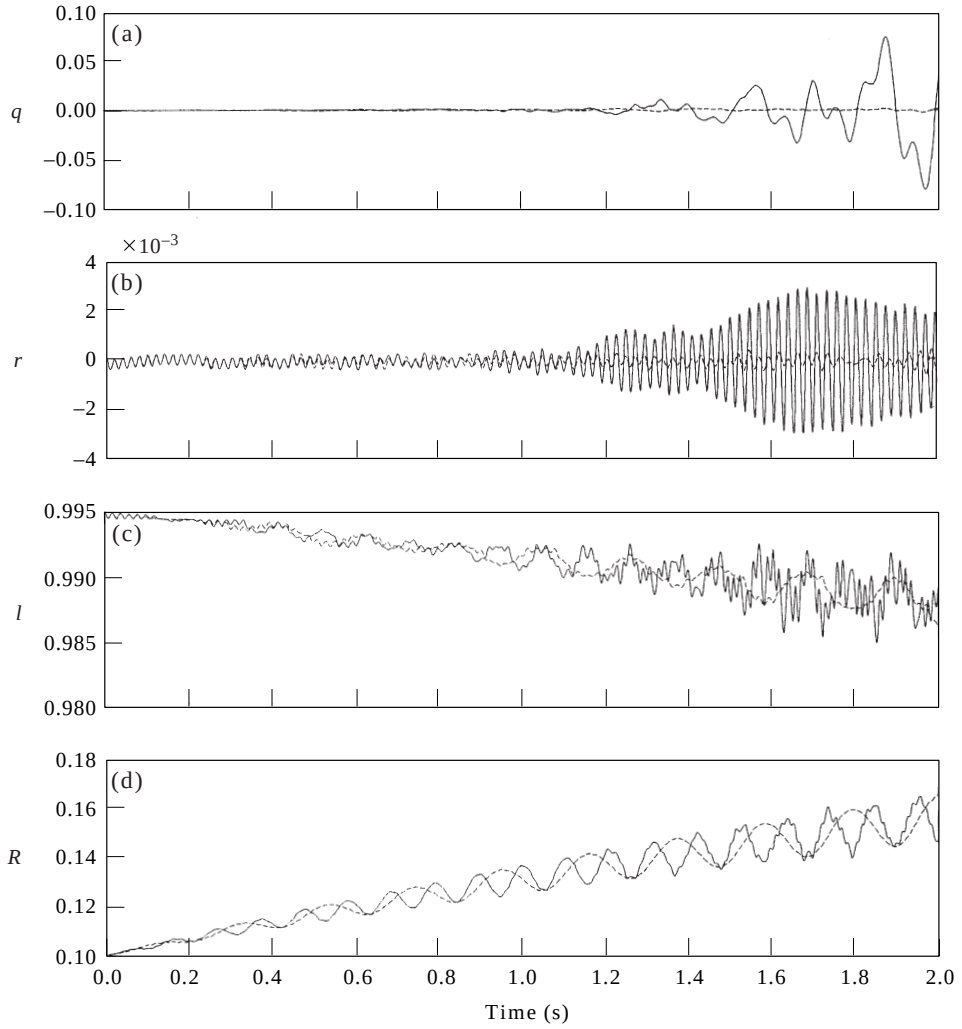

Figure 4. Comparison of dynamic responses by taking the rotary angular velocity $\omega = -10 + 2\cos(\Omega_f t)$, $\Omega_f = \pi c_2/l_0\sqrt{1 - v_0/c_2}$ (– – –) and $\Omega_f = 2\pi c_2/l_0\sqrt{1 - v_0/c_2}$ (——). (a) Middle deflections of the textile. (b) The deflections of the shaft (c) Time-dependent length l of the textile. (d) Time-dependent radius R of the disk.

In Figure 5, we show the compared results of the angular velocity of the rotor, $\omega = -10 + \omega_1 \cos(\Omega_f t)$ by setting $\Omega_f = 2\pi c_2/l_0\sqrt{1 - v_0/c_2}$, $\omega_1 = 1$, 2 and 3. The other parameters are the same as those in Figure 3. Obviously, as the perturbation amplitude ω_1 is larger, the fluctuation is more excited. We note that not only the transient amplitudes of the textile become larger but also the transient deflections of the shaft exhibit beating phenomena.

In Figure 6, we consider the effect of the non-linear term on the textile and rotor. It is observed from Figure 6(a) and (b) that the amplitude is larger and the period of oscillation is shorter when the non-linearity is included. The curves are obtained by making the angular velocity of the rotor equal to -2π and the non-linear terms are $EA = 0$, $100T$ and $900T$. The other parameters are the same as those

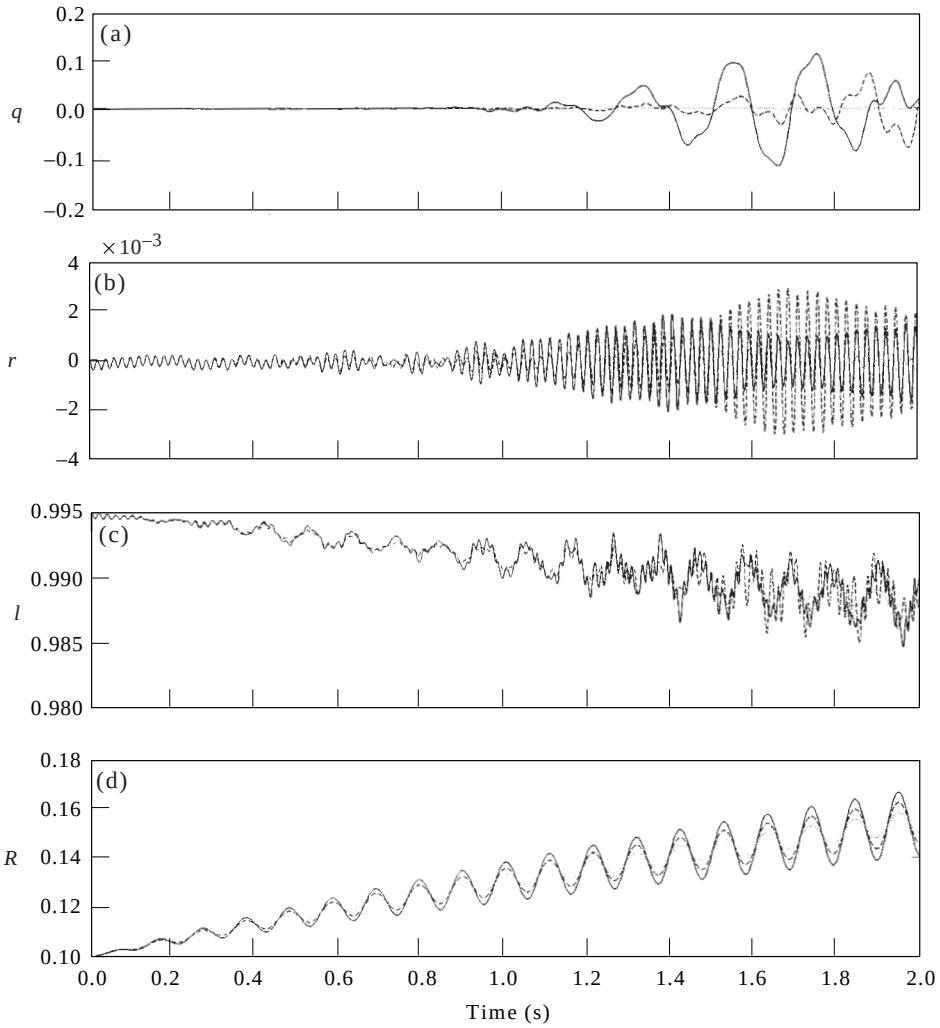

Figure 5. Comparison of dynamic response by taking the rotary angular velocity $\omega = -10 + \omega_1 \cos(\Omega_f t)$, $\Omega_f = 2\pi c_2/l_0\sqrt{1 - v_0/c_2}$, $\omega_1 = 1$ (. . .), $\omega_1 = 2$ (– – –) and $\omega_1 = 3$ (——). (a) Middle deflections of the textile. (b) The deflections of the shaft (c) Time-dependent length l of the textile. (d) Time-dependent radius R of the disk.

in Figure 3. Figure 6(c) shows the time-dependent textile length. Figure 6(d) shows the time-dependent radius of the disk. The radius is the same for the linear and non-linear cases.

5. CONCLUSIONS

In this study, a model of the coupled textile/rotor system that includes the transverse textile vibrations and the rotor whirling has been formulated by Hamilton's principle. However, the application is not straight-forward, since there is a moving boundary and position is not prescribed. In the approximation algorithm, the finite element scheme and Runge–Kutta method are employed to obtain numerical results. We use a variable-size element for which the number of

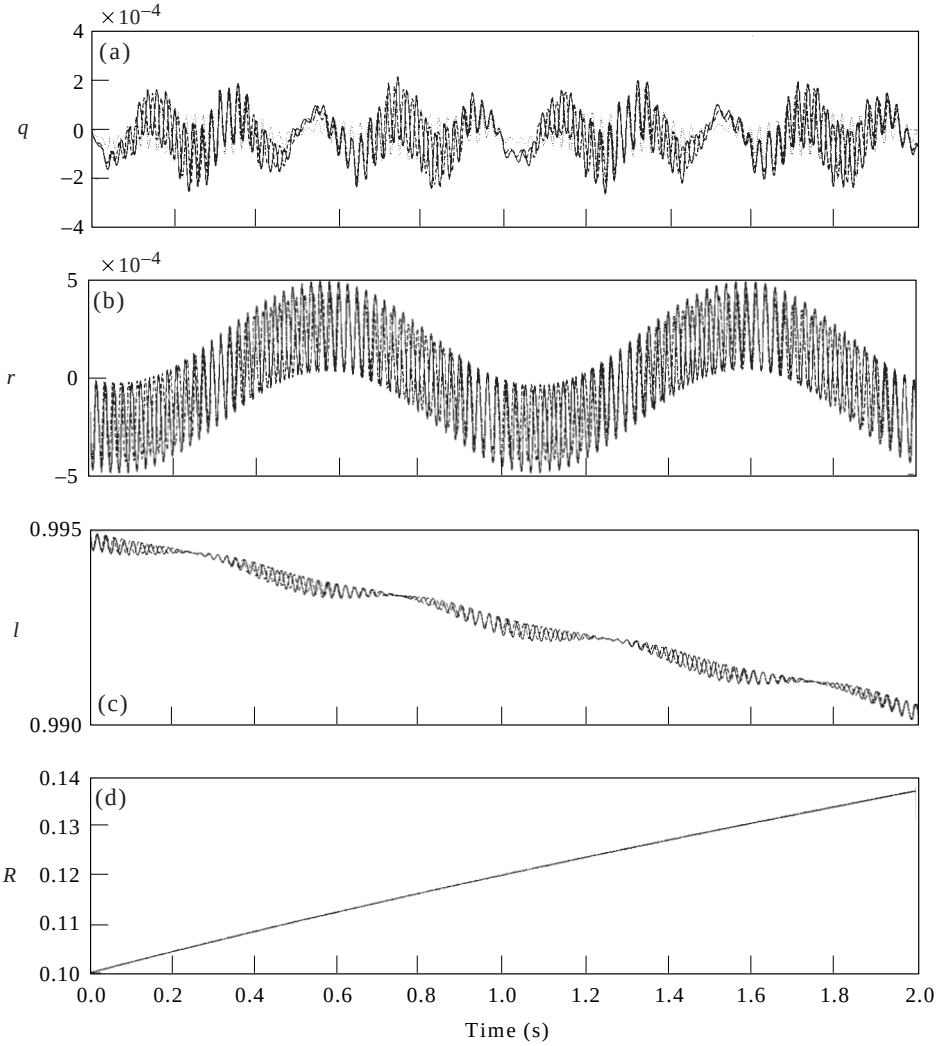

Figure 6. Non-linear effects on the transient textile amplitudes and whirling deflection. $EA = 900T$ (——), $EA = 100T$ (– – –) and $EA = 0$ (. . . .). (a) Middle deflections of the textile. (b) The deflections of the shaft. (c) Time-dependent length l of the textile. (d) Time-dependent radius R of the disk.

elements in the system remains fixed and element size changes with time. The non-constant angular velocity of the rotor and the non-linear terms of the textile are also considered. The time-dependent length of the textile and the radius of the rotor, angular velocity and acceleration are shown for the coupled system.

From the numerical results, we can draw the following conclusions:

(1) The coupled textile/rotor system is a moving boundary problem since the unknown length of the textile has to be determined as a part of the solutions of the governing equations.

(2) If the geometric non-linearity of the textile is neglected for the small-amplitude vibrations, the governing equation of the textile becomes

linear, but the equation for the rotor remains non-linear due to its non-linear boundary at the connection point.

(3) When the effect of the non-linear terms in the textile and rotor are considered, the amplitudes are larger and the periods of oscillations are shorter. We note that both the transient amplitudes of the string and the transient deflections of the shaft exhibit beating phenomena.

(4) For the non-linearity coupled textile/rotor system, the axial travelling speed of the textile has a positive value as it moves along the positive axis direction. In the case of constant angular velocity of the rotor, the radius of the disk and the axial speed of the textile are non-linear functions of time because the rate change of the rotor radius is not equal to zero and axial travelling acceleration also exists.

ACKNOWLEDGMENT

The authors are greatly indebted to the National Science Council R.O.C. for the support of the research through contract No. NSC 88-2212-E-033-002.

REFERENCES

1. S. Nguleswaran and C. J. H. Williams 1967 *International Journal of Mechanism Society* **10**, 239–250. Lateral vibration of band-saw blades, pulley belts and the like.
2. J. A. Elliott 1982 *American Journal of Physics* **50**, 1148–1150. Nonlinearity in vibrating strings.
3. K. Yasuada and T. Torii 1986 *Bulletin of Japan Society of Mechanical Engineers* **29**, 1250–1260. Nonlinear forced oscillations of a string.
4. C. D. Mote Jr 1972 *Shock and Vibration Digest* **4**, 2–11. Dynamic stability of axially moving materials.
5. S. Abrate 1992 *Mechanism and Machine Theory* **27**, 645–659. Vibration of belts and belt drives.
6. T. Kotera and R. Kawai 1988 *Nippon Kikai Gakksi Ronbunshu C Hen* **54**, 9–15. Vibrations of string with time-varying length (2nd Report, free vibrations induced by initial displacements).
7. L. Cveticanin 1986 *Mechanism and Machine Theory* **21**, 29–32. The vibrations of a textile machine rotor with nonlinear characteristics.
8. L. Cveticanin 1991 *Mechanism and Machine Theory* **26**, 253–260. The oscillations of a textile machine rotor on which the textile is wound up.
9. L. Cveticanin 1993 *Journal of Sound and Vibration* **167**, 382–384. The influence of the reactive force on the motion of the rotor on which the band is winding up.
10. L. Cveticanin 1994 *Japan Society Mechanical Engineer International Journal* **37**, 41–48. Dynamic behavior of a rotor with time dependent parameters.
11. A. P. Bessonov 1974 *Osnovji dinamiki mehanizmov speremennojzv zvenjev*. Moskva: Nauka.
12. L. Cveticanin 1984 *Journal of Sound and Vibration* **97**, 181–187. Vibrations of a textile machine rotor.
13. J. M. Vance and J. Lee 1974 *Transactions of the American Society of Mechanical Engineers*, *Journal of Engineering for Industry*, August, 660–668. Stability of high speed rotors with internal friction.
14. Stylanou and Tabarrok 1994 *Journal of Sound and Vibration* **178**(4), 433–453. Finite element analysis of an axially moving beam, Part I: Time integration.
15. Fung and Shieh 1997 *Journal of Sound and Vibration* **199**(2), 207–221. Vibration analysis of a non-linear coupled textile-rotor system with synchronous whirling.

APPENDIX

$$h(t) = \frac{l(t)}{n}, \qquad \dot{h}(t) = \frac{\dot{l}(t)}{n}, \qquad \ddot{h}(t) = \frac{\ddot{l}(t)}{n},$$

$$N = \frac{n}{l(t)}\left[\left(l(t)\frac{j}{n} - x\right)\left(x - l(t)\frac{j-1}{n}\right)\right],$$

$$N_t = \frac{n^2\dot{l}(t)}{l(t)^2}\left[x - l(t)\frac{j}{n} \quad l(t)\frac{j-1}{n} - x\right],$$

$$N_{tt} = \frac{n}{l(t)^3}\left(l(t)\ddot{l}(t) - 2\dot{l}^2(t)\right)\left[l(t)\frac{j}{n} - x \quad x - l(t)\frac{j-1}{n}\right],$$

$$N_{tx} = N_{xt} = \frac{n\dot{l}(t)}{l(t)^2}[1 \quad -1], \qquad B = N_x = \frac{n}{l(t)}[-1 \quad 1],$$

$$[F_{nj}] = \int_{x_j}^{x_{j+1}} -\frac{EA(qB^{\mathrm{T}}BqB^{\mathrm{T}}Bq)}{8}\,\mathrm{d}x = \frac{EA(q(j+1) - q(j))^3}{8h^3(t)}\begin{bmatrix}1\\-1\end{bmatrix},$$

$$\int_{x_j}^{x_{j+1}} (N^{\mathrm{T}}N)\,\mathrm{d}x = \frac{l(t)}{6n}\begin{bmatrix}2 & 1\\1 & 2\end{bmatrix}, \qquad \int_{x_j}^{x_{j+1}} (N_x^{\mathrm{T}}N_x)\,\mathrm{d}x = \frac{n}{l(t)}\begin{bmatrix}-1 & 1\\1 & -1\end{bmatrix},$$

$$\int_{x_j}^{x_{j+1}} (N_x^{\mathrm{T}}N_t)\,\mathrm{d}x = \frac{n\dot{l}(t)}{2l(t)}\begin{bmatrix}1 & 1\\-1 & -1\end{bmatrix}, \qquad \int_{x_j}^{x_{j+1}} (N_t^{\mathrm{T}}N_x)\,\mathrm{d}x = \frac{n\dot{l}(t)}{2l(t)}\begin{bmatrix}1 & -1\\1 & -1\end{bmatrix},$$

$$\int_{x_j}^{x_{j+1}} (N^{\mathrm{T}}N_x)\,\mathrm{d}x = \frac{1}{2}\begin{bmatrix}-1 & 1\\-1 & 1\end{bmatrix}, \qquad \int_{x_j}^{x_{j+1}} (N_x^{\mathrm{T}}N_x)\,\mathrm{d}x = \frac{1}{2}\begin{bmatrix}-1 & -1\\1 & 1\end{bmatrix},$$

$$\int_{x_j}^{x_{j+1}} (N^{\mathrm{T}}N_x)\,\mathrm{d}x = \frac{n\dot{l}(t)}{2l(t)}\begin{bmatrix}-1 & 1\\-1 & 1\end{bmatrix}, \qquad \int_{x_j}^{x_{j+1}} (N_{xt}^{\mathrm{T}}N)\,\mathrm{d}x = \frac{n\dot{l}(t)}{2l(t)}\begin{bmatrix}1 & -1\\1 & -1\end{bmatrix},$$

$$\int_{x_j}^{x_{j+1}} (N^{\mathrm{T}}N_t)\,\mathrm{d}x = \int_{x_j}^{x_{j+1}} (N_t^{\mathrm{T}}N)\,\mathrm{d}x = \frac{-l(t)}{6}\begin{bmatrix}2 & 1\\1 & 2\end{bmatrix},$$

$$\int_{x_j}^{x_{j+1}} (N_{tt}^{\mathrm{T}}N)\,\mathrm{d}x = \frac{(2\dot{l}(t)^2 - l(t)\ddot{l}(t))}{nl(t)}\begin{bmatrix}2 & 1\\1 & 2\end{bmatrix},$$

$$\int_{x_j}^{x_{j+1}} (N_t^{\mathrm{T}}N_t)\,\mathrm{d}x = \frac{n\dot{l}(t)^2}{6l(t)^2}\begin{bmatrix}1 & -1\\-1 & 1\end{bmatrix},$$

$$\int_{x_j}^{x_{j+1}} (xN_x^{\mathrm{T}})\,\mathrm{d}x = \frac{1}{2}\left(\frac{l(t)}{n}\right)(2j-1)\begin{bmatrix}-1\\1\end{bmatrix}, \qquad \int_{x_j}^{x_{j+1}} N^{\mathrm{T}}\,\mathrm{d}x = \frac{l(t)}{2n}\begin{bmatrix}1\\1\end{bmatrix},$$

$$\int_{x_j}^{x_{j+1}} (xN_t^{\mathrm{T}})\,\mathrm{d}x = \frac{n\dot{l}(t)}{6l(t)}\begin{bmatrix} -\left(\frac{l(t)}{n}\right)^2 - 3l(t)^2\left(\frac{j}{n}\right)\left(\frac{j-1}{n}\right) + l(t)^2\left(\frac{j-1}{n}\right)^2 \\ -\left(\frac{l(t)}{n}\right)^2 + l(t)^2\left(\frac{j}{n}\right)\left(\frac{j-1}{n}\right) - l(t)^2\left(\frac{j}{n}\right)^2 \end{bmatrix},$$

$$\int_{x_j}^{x_{j+1}} (xN^{\mathrm{T}})\,\mathrm{d}x = \frac{l(t)^2}{n^2}\begin{bmatrix}(3j-2)\\(3j-1)\end{bmatrix}.$$